Measurement of the $\bar{B}_s^0$ Meson Lifetime in $D_s^+\pi^-$ Decays

R. Aaij *et al.*[*]
(LHCb Collaboration)

(Received 22 July 2014; published 24 October 2014)

We present a measurement of the ratio of the $\bar{B}_s^0$ meson lifetime, in the flavor-specific decay to $D_s^+\pi^-$, to that of the $\bar{B}^0$ meson. The pp collision data used correspond to an integrated luminosity of 1 fb^{-1}, collected with the LHCb detector, at a center-of-mass energy of 7 TeV. Combining our measured value of $1.010 \pm 0.010 \pm 0.008$ for this ratio with the known $\bar{B}^0$ lifetime, we determine the flavor-specific $\bar{B}_s^0$ lifetime to be $\tau(\bar{B}_s^0) = 1.535 \pm 0.015 \pm 0.014$ ps, where the uncertainties are statistical and systematic, respectively. This is the most precise measurement to date, and is consistent with previous measurements and theoretical predictions.

DOI: 10.1103/PhysRevLett.113.172001 PACS numbers: 14.40.Nd, 13.25.Hw, 14.65.Fy

Lifetimes of b-flavored hadrons show the effects of all processes governing their weak decays. In the case of neutral mesons, the decay rates are not purely exponential, but are modified by flavor mixing and charge parity (CP) violation. The $\bar{B}_s^0$ meson's decay width Γ_s differs for the heavy and light mass eigenstates, by an amount $\Delta\Gamma_s$ that has been measured to be significantly different from zero [1]. This gives rise to a rich phenomenology of mixing and CP violation. Precision measurement of the lifetime $\tau_s = \hbar/\Gamma_s$ is therefore an important benchmark. The ratio of $\bar{B}_s^0$ to $\bar{B}^0$ lifetimes is well predicted in the heavy quark expansion model [2], which is used to extract values of the quark-mixing parameters $|V_{cb}|$ and $|V_{ub}|$, and thus lifetime measurements provide a precision test of the theory.

In this Letter we measure the lifetime of the decay $\overset{(-)}{B}{}_s^0 \to D_s^\pm\pi^\mp$ by summing over B_s^0 and $\bar{B}_s^0$ states. Since CP violation in $\bar{B}_s^0$ mixing is negligible [3], the final state receives equal contributions from light and heavy mass eigenstates. Consequently, the decay rate is given by the sum of two exponentials and can be fitted by a single exponential with the measured flavor-specific lifetime $\tau_{\rm fs}$ related to the decay width. Expanding in terms of $\Delta\Gamma_s/\Gamma_s$ [4] (we use natural units where $\hbar = c = 1$),

$$\tau_{\rm fs} \approx \frac{1}{\Gamma_s}\frac{1+(\frac{\Delta\Gamma_s}{2\Gamma_s})^2}{1-(\frac{\Delta\Gamma_s}{2\Gamma_s})^2}. \quad (1)$$

The $\bar{B}_s^0$ time-dependent decay rate is measured with respect to the well-measured lifetimes of the B^- and $\bar{B}^0$ mesons, which are reconstructed in final states with similar topology and kinematic properties. (Reference to a given decay mode implies the use of the charge-conjugate mode as well.)

The LHCb detector [5] is a single-arm forward spectrometer covering the pseudorapidity range $2 < \eta < 5$, designed for the study of particles containing b or c quarks. The detector includes a high-precision tracking system consisting of a silicon-strip vertex detector surrounding the pp interaction region [6], a large-area silicon-strip detector located upstream of a dipole magnet with a bending power of about 4 Tm, and three stations of silicon-strip detectors and straw drift tubes [7] placed downstream of the magnet. The tracking system provides a measurement of momentum p with a relative uncertainty that varies from 0.4% at low momentum to 0.6% at 100 GeV. The minimum distance of a track to a primary vertex, the impact parameter, is measured with a resolution of $(15+29/p_{\rm T})\,\mu$m, where $p_{\rm T}$ is the component of p transverse to the beam, in GeV. Different types of charged hadrons are distinguished using information from two ring-imaging Cherenkov detectors [8]. Photon, electron, and hadron candidates are identified by a calorimeter system consisting of scintillating-pad and preshower detectors, an electromagnetic calorimeter, and a hadronic calorimeter. Muons are identified by a system composed of alternating layers of iron and multiwire proportional chambers [9].

The trigger consists of a hardware stage, based on information from the calorimeter and muon systems, followed by a software stage, which applies a full event reconstruction. The signal candidates are hardware triggered if there is at least one track having a large transverse energy deposit, then the track is required in software to have a transverse momentum $p_{\rm T} > 1.7$ GeV and an impact parameter $\chi^2_{\rm IP}$ with respect to the primary vertex (PV) greater than 16, where $\chi^2_{\rm IP}$ is defined as the difference in χ^2 of a given PV reconstructed with and without the considered particle included. In addition a vertex detached from the PV must be formed with either two, three, or four

[*] Full author list given at the end of the article.

tracks, with a scalar p_T sum of the tracks that must exceed a threshold that varies with the track multiplicity.

The advantage of measuring the $\bar{B}_s^0$ lifetime using the ratio with respect to well-measured lifetimes is that the decay time acceptances introduced by the trigger and selection almost cancel, and only small corrections are required to the ratio of the decay time acceptances, which are taken from simulation. Thus, we reconstruct signals not only in the $\bar{B}_s^0 \to D_s^+\pi^-$, $D_s^+ \to K^+K^-\pi^+$ (denoted $\bar{B}^0_{s[KK\pi]}$) decay mode, but also in the topologically similar channels (i) $B^- \to D^0\pi^-$, $D^0 \to K^-\pi^+$ ($B^-_{[K\pi]}$), (ii) $B^- \to D^0\pi^-$, $D^0 \to K^-\pi^-\pi^+\pi^+$ ($B^-_{[K\pi\pi\pi]}$), and (iii) $\bar{B}^0 \to D^+\pi^-$, $D^+ \to K^-\pi^+\pi^+$ ($\bar{B}^0_{[K\pi\pi]}$).

These decay modes are selected using some common criteria. All of the tracks coming from candidate D meson decays are required to have $\chi^2_{\rm IP} > 9$. Pions arising from $\bar{B}$ meson decays have a more selective requirement $\chi^2_{\rm IP} > 36$ and they are required to be inconsistent with being identified as muons. The D candidates are required to have masses within 25 MeV of their known values [1], which corresponds to about 3 rms widths, be reconstructed downstream of the PV, and have $\chi^2_{\rm IP} > 4$. The D vertex separation from the $\bar{B}$ vertex should satisfy $\chi^2_{\rm VS} > 2$, where $\chi^2_{\rm VS}$ is the increase in χ^2 of the parent $\bar{B}$ vertex fit when the D decay products are constrained to come from the $\bar{B}$ vertex, relative to when they are allowed to come from a separate vertex.

B^- and $\bar{B}^0$ candidates are required to have $\chi^2_{\rm IP} < 16$ with respect to the PV and masses in the ranges 5100–5600 MeV, while for $\bar{B}_s^0$ candidates the mass range is changed to 5200–5700 MeV. The cosine of the angle between the $\bar{B}$ momentum and its direction of flight is required to be greater than 0.9999. All signal candidates are refitted taking both D mass and vertex constraints into account [10]. All charged particles are required to be identified as either pions or kaons. Efficiencies are evaluated with a data-driven method using large samples of $D^0 \to K^-\pi^+$ events, where the kinematic distributions of kaons and pions from the calibration sample are reweighted to match those of the $\bar{B}$ decays under study.

We eliminate $\bar{B}^0_{[K\pi\pi]}$ decay candidates that result from other similar decays, the $\bar{B}_s^0 \to D_s^+\pi^-$, $D_s^+ \to K^+K^-\pi^+$ and $\Lambda_b^0 \to \Lambda_c^+\pi^-$, $\Lambda_c^+ \to pK^-\pi^+$ modes, if the invariant mass of the particles forming the D^+ candidate, with appropriately swapped mass assignments, is compatible within 30 MeV with either of the known D_s^+ or Λ_c^+ masses. Similar vetoes are applied for $\bar{B}^0_{s[KK\pi]}$ candidates, where cross feed from $\bar{B}^0 \to D^+\pi^-$, $D^+ \to K^-\pi^+\pi^+$, and $\Lambda_b^0 \to \Lambda_c^+\pi^-$, $\Lambda_c^+ \to pK^-\pi^+$ can happen if misidentification occurs. The combined efficiencies of the particle identification requirements and the mass vetoes depend on the specific decay mode considered, ranging from 80% to 90%, while more than 95% of cross-feed backgrounds are rejected.

The $\bar{B}$ candidate mass distributions for the four decay modes considered are shown in Fig. 1, along with the

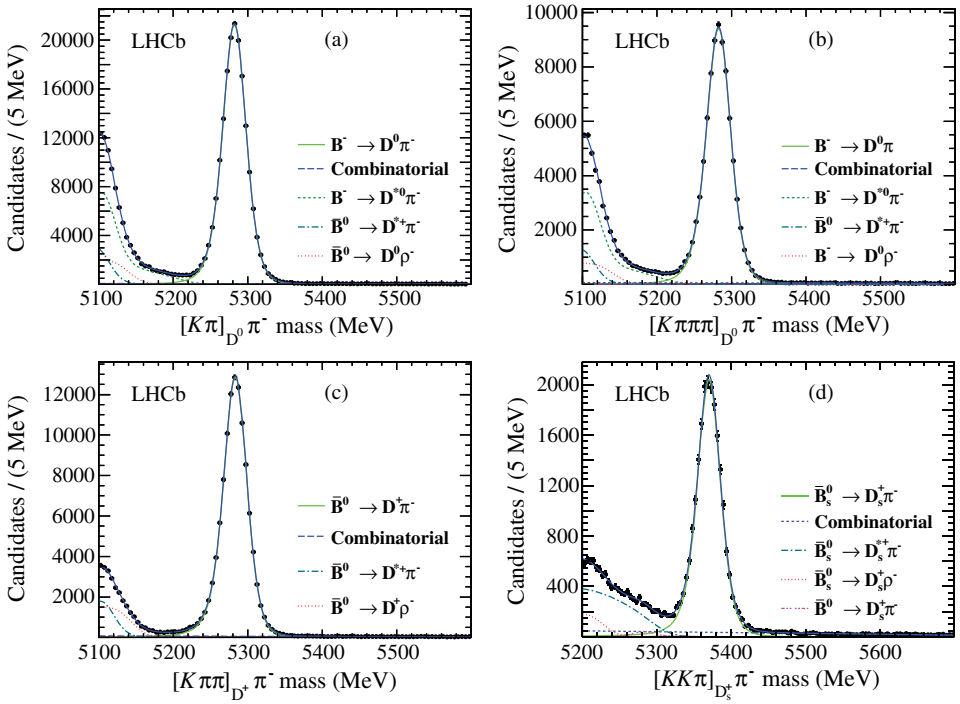

FIG. 1 (color online). Fits to the invariant mass spectra of candidates for the decays (a) $B^- \to D^0[K\pi]\pi^-$, (b) $B^- \to D^0[K\pi\pi\pi]\pi^-$, (c) $\bar{B}^0 \to D^+[K\pi\pi]\pi^-$, (d) $\bar{B}_s^0 \to D_s^+[KK\pi]\pi^-$. The points are the data and the superimposed curves show the fit components. The solid (blue) curve gives the total. The DK^- component is not visible, but is included.

results of binned maximum likelihood fits. Signal shapes are parametrized using modified Gaussian functions (Cruijff) with independent tail shapes on both sides [11]. All signal parameters are allowed to vary in the fit. A residual component of $\bar{B} \to DK^-$ misidentified events is also included, with its yield constrained to that determined by examining the data where the kaon is positively identified instead of the pion. Partially reconstructed backgrounds, where a pion or a photon is missed in reconstruction, are modeled using a sum of parametric empirical functions convolved with resolution functions. The unique decay kinematics of each of the modes, mostly determined by the polarization amplitudes, is taken into account. The combinatorial background is parametrized by a linear term. The fitted signal yields are $179\,623 \pm 467$, $82\,880 \pm 339$, $109\,670 \pm 378$ and $21\,058 \pm 245$ for $B^-_{[K\pi]}$, $B^-_{[K\pi\pi\pi]}$, $\bar{B}^0_{[K\pi\pi]}$, and $\bar{B}^0_{s[KK\pi]}$ decays, respectively.

The decay time t is derived from a flight-length measurement between production and decay points of the $\bar{B}$ particle, given by

$$t = m\frac{\vec{d}\cdot\vec{p}}{|p|^2}, \tag{2}$$

where m is the reconstructed invariant mass, $\vec{p}$ is the momentum. and $\vec{d}$ is the distance vector of the particle from its production to decay vertices. Prior to this determination, the PV position is refitted excluding the tracks forming the signal candidate, and the $\bar{B}$ meson is further constrained to come from the PV. The decay time distribution of the signal $D_T(t)$ can be described by an exponential function convolved with a decay time resolution function $G(t,\sigma)$, and multiplied by an acceptance function $A(t)$:

$$D_T(t) = A(t) \times [e^{-t'/\tau} \otimes G(t-t',\sigma)]. \tag{3}$$

The ratio of the measured decay time distributions of $\bar{B}^0_s$ to $\bar{B}^0$ or B^- (we denote the use of either $\bar{B}^0$ or B^- modes by the symbol B_x) can be written as

$$R(t) = \frac{A_{\bar{B}^0_s}(t) \times [e^{-t'/\tau_{\bar{B}^0_s}} \otimes G(t-t',\sigma_{\bar{B}^0_s})]}{A_{B_x}(t) \times [e^{-t'/\tau_{B_x}} \otimes G(t-t',\sigma_{B_x})]}. \tag{4}$$

Resolutions are evaluated using simulated events and they are found to be 38, 37, 39, and 36 fs for $\bar{B}^0_{s[KK\pi]}$, $\bar{B}^0_{[K\pi\pi]}$, $B^-_{[K\pi]}$, and $B^-_{[K\pi\pi\pi]}$, respectively. Since the resolution is very similar in all the modes, and much smaller than our 0.5 ps bin width, the resolution effects cancel [12], and we are left with a ratio of two exponentials times the ratio of acceptance functions,

$$R(t) = \frac{A_{\bar{B}^0_s}(t)}{A_{B_x}(t)} e^{-t(1/\tau_{\bar{B}^0_s} - 1/\tau_{B_x})} = \frac{A_{\bar{B}^0_s}(t)}{A_{B_x}(t)} e^{-t\Delta_{\bar{B}^0_s B_x}}, \tag{5}$$

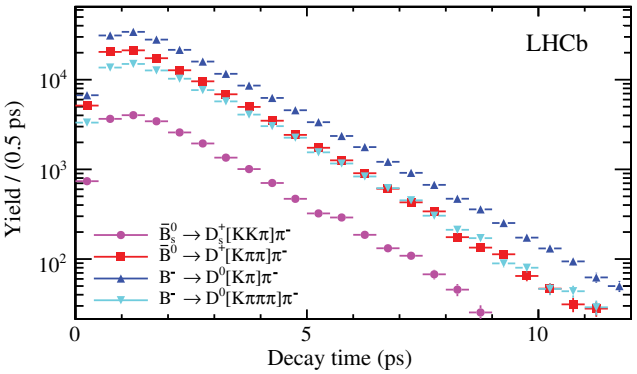

FIG. 2 (color online). Decay time distributions for $B^- \to \bar{D}^0[K\pi]\pi^-$ shown as triangles (blue), $B^- \to D^0[K\pi\pi\pi]\pi^-$ shown as inverted triangles (cyan), $B^0 \to D^+[K\pi\pi]\pi^-$ shown as squares (red), $\bar{B}^0_s \to D^+_s[KK\pi]\pi^-$ shown as circles (magenta). For most entries the error bars are smaller than the point markers.

where $\Delta_{\bar{B}^0_s B_x} \equiv 1/\tau_{\bar{B}^0_s} - 1/\tau_{B_x}$. Acceptance functions are evaluated by simulation. The effective lifetime $\tau_{\bar{B}^0_s}$ can then be calculated from $\Delta_{\bar{B}^0_s B_x}$ using the well-known B_x lifetimes. The current world average values are $\tau_{\bar{B}^0} = 1.519 \pm 0.007$ ps and $\tau_{B^-} = 1.641 \pm 0.008$ ps [1].

The signal yields are determined in each decay time bin by fitting the mass distribution in each bin with the same shapes as used in the full fits, with the signal shape parameters fixed to those of the full fit as they are independent of the decay time. The yields are shown in Fig. 2.

The signal yields are then corrected by the relative decay time acceptance ratio, obtained by simulation, and shown in Fig. 3. Then the efficiency-corrected yield ratios are fitted with a single exponential function to extract $\Delta_{\bar{B}^0_s B_x}$. Fits are performed in the 1–8 ps region. The 0–1 ps region is excluded since the ratio of acceptances varies significantly

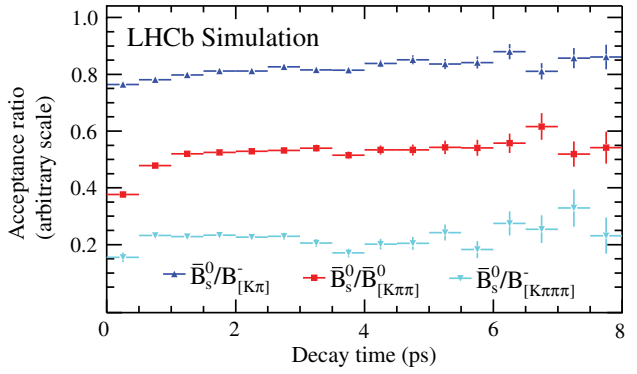

FIG. 3 (color online). Ratio of the decay time acceptances between $\bar{B}^0_s \to D^+_s[KK\pi]\pi^-$ and $B^- \to D^0[K\pi]\pi^-$ shown as triangles (blue), $B^0 \to D^+[K\pi\pi]\pi^-$ shown as squares (red), and $B^- \to \bar{D}^0[K\pi\pi\pi]\pi^-$ shown as inverted triangles (cyan). The vertical axis is shown in an arbitrary scale, different for each mode ratio to improve clarity.

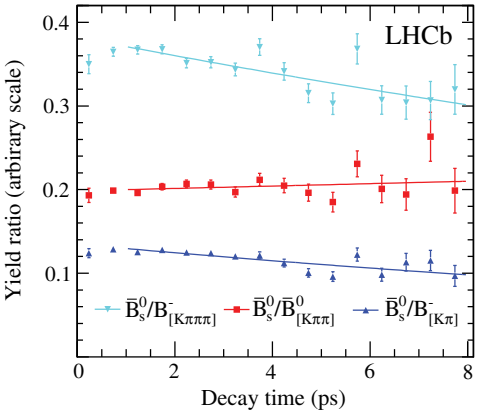

FIG. 4 (color online). Efficiency-corrected yield ratios of $\bar{B}^0_s \to D^+_s[KK\pi]\pi^-$ relative to $B^- \to D^0[K\pi]\pi^-$ shown as triangles (blue), $\bar{B}^0 \to D^+[K\pi\pi]\pi^-$ shown as squares (red), and $B^- \to D^0[K\pi\pi\pi]\pi^-$ shown as inverted triangles (cyan). The simulation uncertainties are not included. The exponential fits are also shown. The vertical axis is shown in an arbitrary scale, different for each case to improve clarity.

here, due to the differences between the lifetimes and track multiplicities in the D decays.

The full analysis is also applied to the control decay modes and the B^- lifetime is measured relative to that of the $\bar{B}^0$ meson. Given their well-known lifetimes, this provides a robust check on the validity of the procedure. We then measure the $\bar{B}^0_s/B_y$ lifetime ratio for each of the three samples. The exponential fits for the $\bar{B}^0_s/B_y$ lifetime ratios are shown in Fig. 4, with the results given in Table I. In each case good agreement with the known values of the light $\bar{B}$ meson lifetime ratio is found, and the three values of the $\bar{B}^0_s$ lifetime are consistent.

The sources of systematic uncertainties on $\Delta_{\bar{B}^0_s B_x}$ are summarized in Table II. The statistical precision on the relative acceptance is the largest source of systematic uncertainty. The uncertainties due to the background description are estimated by comparing the nominal result to that obtained when the linear background slope is allowed to float separately in each decay time bin; in addition, an exponential shape is used, and the largest deviation is assigned as a systematic uncertainty. Using a different signal shape to fit the data (double Crystal Ball function [13]) leads to small changes. There is also an uncertainty due to the decay time range and binning used. These uncertainties are ascertained by changing the fit range limits down to 0.5 ps and changing the size of the bins from 0.3 to 1 ps. The relative measurements with respect to the three control samples agree within 0.005 ps, and this is conservatively added to the total systematic uncertainty.

TABLE II. Systematic uncertainties for $\Delta_{\bar{B}^0_s B_x}$ (ps^{-1}).

Source	$\bar{B}^0_{s[KK\pi]}/B^-_{[K\pi]}$	$\bar{B}^0_{s[KK\pi]}/\bar{B}^0_{[K\pi\pi]}$	$\bar{B}^0_{s[KK\pi]}/B^-_{[K\pi\pi\pi]}$
Lifetime acceptance	0.003	0.004	0.005
Background model	0.002	0.002	0.002
Signal shape	0.0004	0.0005	0.0005
Binning schemes	0.003	0.001	0.005
Total	0.005	0.005	0.007

Using the known lifetimes of the B^- and $\bar{B}^0$ mesons and the three different normalization channels, the flavor-specific $\bar{B}^0_s$ lifetime is determined as

$$\tau_{\mathrm{fs}} = 1.540 \pm 0.015 \pm 0.012 \pm 0.008\ \mathrm{ps}[B^-_{[K\pi]}]$$

$$\tau_{\mathrm{fs}} = 1.535 \pm 0.015 \pm 0.012 \pm 0.007\ \mathrm{ps}[\bar{B}^0_{[K\pi\pi]}]$$

$$\tau_{\mathrm{fs}} = 1.535 \pm 0.016 \pm 0.018 \pm 0.008\ \mathrm{ps}[B^-_{[K\pi\pi\pi]}],$$

where the first uncertainty is statistical, the second is systematic and the third is the uncertainty due to the input decay lifetimes of the B^- and $\bar{B}^0$ mesons, 0.008 ps for the B^- meson and 0.007 ps for the B^0 meson [1]. As the results are fully correlated, that with the smallest uncertainty is chosen

$$\tau_{\mathrm{fs}} = 1.535 \pm 0.015 \pm 0.012 \pm 0.007\ \mathrm{ps}.$$

TABLE I. Measured lifetime ratios, compared with the known values, and the difference (fitted minus known), as well as the resulting measured lifetime τ_{meas}. Errors are statistical only. B_x and B_y indicate the modes used.

Value	$B^-_{[K\pi]}/\bar{B}^0_{[K\pi\pi]}$	$B^-_{[K\pi\pi\pi]}/\bar{B}^0_{[K\pi\pi]}$	$B^-_{[K\pi\pi\pi]}/B^-_{[K\pi]}$
Measured $\Delta_{B_x B_y}$ (ps^{-1})	-0.0451 ± 0.0033	-0.0452 ± 0.0039	0.0011 ± 0.0034
Known $\Delta_{B_x B_y}$ (ps^{-1}) [1]	-0.0489 ± 0.0042	-0.0489 ± 0.0042	0
Difference (ps^{-1})	0.0038 ± 0.0054	0.0037 ± 0.0057	0.0011 ± 0.0034
$\tau_{\mathrm{meas}}(B^-)$ (ps)	1.631 ± 0.009	1.631 ± 0.010	1.638 ± 0.009

Value	$\bar{B}^0_{s[KK\pi]}/B^-_{[K\pi]}$	$\bar{B}^0_{s[KK\pi]}/\bar{B}^0_{[K\pi\pi]}$	$\bar{B}^0_{s[KK\pi]}/B^-_{[K\pi\pi\pi]}$
Fitted $\Delta_{\bar{B}^0_s B_y}$ (ps^{-1})	0.0402 ± 0.0062	$-0.0063 \pm 0.006\,5$	0.0418 ± 0.0066
τ_{B_y} (ps) [1]	1.641 ± 0.008	1.519 ± 0.007	1.641 ± 0.008
$\tau_{\mathrm{meas}}(\bar{B}^0_s)$ (ps)	1.540 ± 0.015	1.535 ± 0.015	1.535 ± 0.016

This is the most precise measurement to date and it is consistent with previously available flavor-specific measurements [14], and measurements of $\bar{B}_s^0$ lifetimes in CP eigenstate modes [15]. The lifetime ratio $\tau_{\rm fs}(\bar{B}_s^0)/\tau(\bar{B}^0) = 1/(1+\tau(\bar{B}^0)\Delta_{\bar{B}_s^0 B^0})$ is determined as $1.010 \pm 0.010 \pm 0.008$, where we assign the uncertainty due to the $\bar{B}^0$ lifetime as purely systematic. A rather precise prediction of Γ_d/Γ_s is given using the heavy quark expansion model [2]. To compare with our measured lifetime ratio we apply a 0.8% correction from Eq. (1), resulting in a corrected prediction for our measured lifetime ratio of 1.009 ± 0.004, in excellent agreement with our measurement, lending credence to this model.

We express our gratitude to our colleagues in the CERN accelerator departments for the excellent performance of the LHC. We thank the technical and administrative staff at the LHCb institutes. We acknowledge support from CERN and from the national agencies: CAPES, CNPq, FAPERJ, and FINEP (Brazil); NSFC (China); CNRS/IN2P3 (France); BMBF, DFG, HGF, and MPG (Germany); SFI (Ireland); INFN (Italy); FOM and NWO (The Netherlands); MNiSW and NCN (Poland); MEN/IFA (Romania); MinES and FANO (Russia); MinECo (Spain); SNSF and SER (Switzerland); NASU (Ukraine); STFC (United Kingdom); NSF (USA). The Tier1 computing centres are supported by IN2P3 (France), KIT and BMBF (Germany), INFN (Italy), NWO and SURF (The Netherlands), PIC (Spain), and GridPP (United Kingdom). We are indebted to the communities behind the multiple open source software packages on which we depend. We are also thankful for the computing resources and the access to software R&D tools provided by Yandex LLC (Russia). Individual groups or members have received support from EPLANET, Marie Skłodowska-Curie Actions, and ERC (European Union), Conseil général de Haute-Savoie, Labex ENIGMASS, and OCEVU, Région Auvergne (France), RFBR (Russia), XuntaGal, and GENCAT (Spain), and the Royal Society and Royal Commission for the Exhibition of 1851 (United Kingdom).

[1] See J. Beringer *et al.* (Particle Data Group), Phys. Rev. D **86**, 010001 (2012), and the 2013 partial update for the 2014 edition.
[2] A. Lenz, arXiv:1405.3601.
[3] R. Aaij *et al.* (LHCb collaboration), Phys. Lett. B **728**, 607 (2014).
[4] K. Hartkorn and H. Moser, Eur. Phys. J. C **8**, 381 (1999).
[5] A. A. Alves, Jr. *et al.* (LHCb Collaboration), JINST **3**, S08005 (2008).
[6] R. Aaij *et al.*, JINST **9**, P09007 (2014).
[7] R. Arink *et al.*, JINST **9**, P01002 (2014),
[8] M. Adinolfi *et al.*, Eur. Phys. J. C **73**, 2431 (2013).
[9] A. A. Alves, Jr. *et al.*, JINST **8**, P02022 (2013).
[10] W. D. Hulsbergen, Nucl. Instrum. Methods Phys. Res., Sect. A **552**, 566 (2005);
[11] R. Aaij *et al.* (LHCb Collaboration), Phys. Lett. B **718**, 902 (2013); P. del Amo Sanchez *et al.* (*BABAR* Collaboration), Phys. Rev. D **82**, 051101 (2010).
[12] R. Aaij *et al.* (LHCb Collaboration), Phys. Lett. B **734**, 122 (2014).
[13] T. Skwarnicki, Ph.D. thesis, Institute of Nuclear Physics, Krakow, [DESY-F31-86-02, 1986].
[14] T. Aaltonen *et al.* (CDF Collaboration), Phys. Rev. Lett. **107**, 272001 (2011); R. Aaij *et al.* (LHCb Collaboration), Phys. Rev. Lett. **112**, 111802 (2014); P. Abreu *et al.* (DELPHI Collaboration), Eur. Phys. J. C **16**, 555 (2000); K. Ackerstaff *et al.* (OPAL Collaboration), Phys. Lett. B **426**, 161 (1998); D. Buskulic *et al.* (ALEPH Collaboration), Phys. Lett. B **377**, 205 (1996).
[15] S. Stone, 2014 Flavor Physics and CP Violation (FPCP 2014), Marseille, France, May 26–30, 2014, arXiv:1406.6497 (to be published in the conference proceedings).

R. Aaij,[41] B. Adeva,[37] M. Adinolfi,[46] A. Affolder,[52] Z. Ajaltouni,[5] S. Akar,[6] J. Albrecht,[9] F. Alessio,[38] M. Alexander,[51] S. Ali,[41] G. Alkhazov,[30] P. Alvarez Cartelle,[37] A. A. Alves Jr.,[25,38] S. Amato,[2] S. Amerio,[22] Y. Amhis,[7] L. An,[3] L. Anderlini,[17,a] J. Anderson,[40] R. Andreassen,[57] M. Andreotti,[16,b] J. E. Andrews,[58] R. B. Appleby,[54] O. Aquines Gutierrez,[10] F. Archilli,[38] A. Artamonov,[35] M. Artuso,[59] E. Aslanides,[6] G. Auriemma,[25,c] M. Baalouch,[5] S. Bachmann,[11] J. J. Back,[48] A. Badalov,[36] W. Baldini,[16] R. J. Barlow,[54] C. Barschel,[38] S. Barsuk,[7] W. Barter,[47] V. Batozskaya,[28] V. Battista,[39] A. Bay,[39] L. Beaucourt,[4] J. Beddow,[51] F. Bedeschi,[23] I. Bediaga,[1] S. Belogurov,[31] K. Belous,[35] I. Belyaev,[31] E. Ben-Haim,[8] G. Bencivenni,[18] S. Benson,[38] J. Benton,[46] A. Berezhnoy,[32] R. Bernet,[40] M.-O. Bettler,[47] M. van Beuzekom,[41] A. Bien,[11] S. Bifani,[45] T. Bird,[54] A. Bizzeti,[17,d] P. M. Bjørnstad,[54] T. Blake,[48] F. Blanc,[39] J. Blouw,[10] S. Blusk,[59] V. Bocci,[25] A. Bondar,[34] N. Bondar,[30,38] W. Bonivento,[15,38] S. Borghi,[54] A. Borgia,[59] M. Borsato,[7] T. J. V. Bowcock,[52] E. Bowen,[40] C. Bozzi,[16] T. Brambach,[9] J. van den Brand,[42] J. Bressieux,[39] D. Brett,[54] M. Britsch,[10] T. Britton,[59] J. Brodzicka,[54] N. H. Brook,[46] H. Brown,[52] A. Bursche,[40] G. Busetto,[22,e] J. Buytaert,[38] S. Cadeddu,[15] R. Calabrese,[16,b] M. Calvi,[20,f] M. Calvo Gomez,[36,g] P. Campana,[18,38] D. Campora Perez,[38] A. Carbone,[14,h] G. Carboni,[24,i] R. Cardinale,[19,38,j] A. Cardini,[15] L. Carson,[50] K. Carvalho Akiba,[2] G. Casse,[52] L. Cassina,[20]

L. Castillo Garcia,[38] M. Cattaneo,[38] Ch. Cauet,[9] R. Cenci,[58] M. Charles,[8] Ph. Charpentier,[38] M. Chefdeville,[4] S. Chen,[54] S.-F. Cheung,[55] N. Chiapolini,[40] M. Chrzaszcz,[40,26] K. Ciba,[38] X. Cid Vidal,[38] G. Ciezarek,[53] P. E. L. Clarke,[50] M. Clemencic,[38] H. V. Cliff,[47] J. Closier,[38] V. Coco,[38] J. Cogan,[6] E. Cogneras,[5] P. Collins,[38] A. Comerma-Montells,[11] A. Contu,[15] A. Cook,[46] M. Coombes,[46] S. Coquereau,[8] G. Corti,[38] M. Corvo,[16,b] I. Counts,[56] B. Couturier,[38] G. A. Cowan,[50] D. C. Craik,[48] M. Cruz Torres,[60] S. Cunliffe,[53] R. Currie,[50] C. D'Ambrosio,[38] J. Dalseno,[46] P. David,[8] P. N. Y. David,[41] A. Davis,[57] K. De Bruyn,[41] S. De Capua,[54] M. De Cian,[11] J. M. De Miranda,[1] L. De Paula,[2] W. De Silva,[57] P. De Simone,[18] D. Decamp,[4] M. Deckenhoff,[9] L. Del Buono,[8] N. Déléage,[4] D. Derkach,[55] O. Deschamps,[5] F. Dettori,[38] A. Di Canto,[38] H. Dijkstra,[38] S. Donleavy,[52] F. Dordei,[11] M. Dorigo,[39] A. Dosil Suárez,[37] D. Dossett,[48] A. Dovbnya,[43] K. Dreimanis,[52] G. Dujany,[54] F. Dupertuis,[39] P. Durante,[38] R. Dzhelyadin,[35] A. Dziurda,[26] A. Dzyuba,[30] S. Easo,[49,38] U. Egede,[53] V. Egorychev,[31] S. Eidelman,[34] S. Eisenhardt,[50] U. Eitschberger,[9] R. Ekelhof,[9] L. Eklund,[51] I. El Rifai,[5] Ch. Elsasser,[40] S. Ely,[59] S. Esen,[11] H.-M. Evans,[47] T. Evans,[55] A. Falabella,[14] C. Färber,[11] C. Farinelli,[41] N. Farley,[45] S. Farry,[52] R. Fay,[52] D. Ferguson,[50] V. Fernandez Albor,[37] F. Ferreira Rodrigues,[1] M. Ferro-Luzzi,[38] S. Filippov,[33] M. Fiore,[16,b] M. Fiorini,[16,b] M. Firlej,[27] C. Fitzpatrick,[39] T. Fiutowski,[27] M. Fontana,[10] F. Fontanelli,[19,j] R. Forty,[38] O. Francisco,[2] M. Frank,[38] C. Frei,[38] M. Frosini,[17,38,a] J. Fu,[21,38] E. Furfaro,[24,i] A. Gallas Torreira,[37] D. Galli,[14,h] S. Gallorini,[22] S. Gambetta,[19,j] M. Gandelman,[2] P. Gandini,[59] Y. Gao,[3] J. García Pardiñas,[37] J. Garofoli,[59] J. Garra Tico,[47] L. Garrido,[36] C. Gaspar,[38] R. Gauld,[55] L. Gavardi,[9] G. Gavrilov,[30] E. Gersabeck,[11] M. Gersabeck,[54] T. Gershon,[48] Ph. Ghez,[4] A. Gianelle,[22] S. Giani',[39] V. Gibson,[47] L. Giubega,[29] V. V. Gligorov,[38] C. Göbel,[60] D. Golubkov,[31] A. Golutvin,[53,31,38] A. Gomes,[1,k] C. Gotti,[20] M. Grabalosa Gándara,[5] R. Graciani Diaz,[36] L. A. Granado Cardoso,[38] E. Graugés,[36] G. Graziani,[17] A. Grecu,[29] E. Greening,[55] S. Gregson,[47] P. Griffith,[45] L. Grillo,[11] O. Grünberg,[62] B. Gui,[59] E. Gushchin,[33] Yu. Guz,[35,38] T. Gys,[38] C. Hadjivasiliou,[59] G. Haefeli,[39] C. Haen,[38] S. C. Haines,[47] S. Hall,[53] B. Hamilton,[58] T. Hampson,[46] X. Han,[11] S. Hansmann-Menzemer,[11] N. Harnew,[55] S. T. Harnew,[46] J. Harrison,[54] J. He,[38] T. Head,[38] V. Heijne,[41] K. Hennessy,[52] P. Henrard,[5] L. Henry,[8] J. A. Hernando Morata,[37] E. van Herwijnen,[38] M. Heß,[62] A. Hicheur,[1] D. Hill,[55] M. Hoballah,[5] C. Hombach,[54] W. Hulsbergen,[41] P. Hunt,[55] N. Hussain,[55] D. Hutchcroft,[52] D. Hynds,[51] M. Idzik,[27] P. Ilten,[56] R. Jacobsson,[38] A. Jaeger,[11] J. Jalocha,[55] E. Jans,[41] P. Jaton,[39] A. Jawahery,[58] F. Jing,[3] M. John,[55] D. Johnson,[55] C. R. Jones,[47] C. Joram,[38] B. Jost,[38] N. Jurik,[59] M. Kaballo,[9] S. Kandybei,[43] W. Kanso,[6] M. Karacson,[38] T. M. Karbach,[38] S. Karodia,[51] M. Kelsey,[59] I. R. Kenyon,[45] T. Ketel,[42] B. Khanji,[20] C. Khurewathanakul,[39] S. Klaver,[54] K. Klimaszewski,[28] O. Kochebina,[7] M. Kolpin,[11] I. Komarov,[39] R. F. Koopman,[42] P. Koppenburg,[41,38] M. Korolev,[32] A. Kozlinskiy,[41] L. Kravchuk,[33] K. Kreplin,[11] M. Kreps,[48] G. Krocker,[11] P. Krokovny,[34] F. Kruse,[9] W. Kucewicz,[26,l] M. Kucharczyk,[20,26,38,f] V. Kudryavtsev,[34] K. Kurek,[28] T. Kvaratskheliya,[31] V. N. La Thi,[39] D. Lacarrere,[38] G. Lafferty,[54] A. Lai,[15] D. Lambert,[50] R. W. Lambert,[42] G. Lanfranchi,[18] C. Langenbruch,[48] B. Langhans,[38] T. Latham,[48] C. Lazzeroni,[45] R. Le Gac,[6] J. van Leerdam,[41] J.-P. Lees,[4] R. Lefèvre,[5] A. Leflat,[32] J. Lefrançois,[7] S. Leo,[23] O. Leroy,[6] T. Lesiak,[26] B. Leverington,[11] Y. Li,[3] T. Likhomanenko,[63] M. Liles,[52] R. Lindner,[38] C. Linn,[38] F. Lionetto,[40] B. Liu,[15] S. Lohn,[38] I. Longstaff,[51] J. H. Lopes,[2] N. Lopez-March,[39] P. Lowdon,[40] H. Lu,[3] D. Lucchesi,[22,e] H. Luo,[50] A. Lupato,[22] E. Luppi,[16,b] O. Lupton,[55] F. Machefert,[7] I. V. Machikhiliyan,[31] F. Maciuc,[29] O. Maev,[30] S. Malde,[55] A. Malinin,[63] G. Manca,[15,m] G. Mancinelli,[6] J. Maratas,[5] J. F. Marchand,[4] U. Marconi,[14] C. Marin Benito,[36] P. Marino,[23,n] R. Märki,[39] J. Marks,[11] G. Martellotti,[25] A. Martens,[8] A. Martín Sánchez,[7] M. Martinelli,[39] D. Martinez Santos,[42] F. Martinez Vidal,[64] D. Martins Tostes,[2] A. Massafferri,[1] R. Matev,[38] Z. Mathe,[38] C. Matteuzzi,[20] A. Mazurov,[16,b] M. McCann,[53] J. McCarthy,[45] A. McNab,[54] R. McNulty,[12] B. McSkelly,[52] B. Meadows,[57] F. Meier,[9] M. Meissner,[11] M. Merk,[41] D. A. Milanes,[8] M.-N. Minard,[4] N. Moggi,[14] J. Molina Rodriguez,[60] S. Monteil,[5] M. Morandin,[22] P. Morawski,[27] A. Mordà,[6] M. J. Morello,[23,n] J. Moron,[27] A.-B. Morris,[50] R. Mountain,[59] F. Muheim,[50] K. Müller,[40] M. Mussini,[14] B. Muster,[39] P. Naik,[46] T. Nakada,[39] R. Nandakumar,[49] I. Nasteva,[2] M. Needham,[50] N. Neri,[21] S. Neubert,[38] N. Neufeld,[38] M. Neuner,[11] A. D. Nguyen,[39] T. D. Nguyen,[39] C. Nguyen-Mau,[39,o] M. Nicol,[7] V. Niess,[5] R. Niet,[9] N. Nikitin,[32] T. Nikodem,[11] A. Novoselov,[35] D. P. O'Hanlon,[48] A. Oblakowska-Mucha,[27] V. Obraztsov,[35] S. Oggero,[41] S. Ogilvy,[51] O. Okhrimenko,[44] R. Oldeman,[15,m] G. Onderwater,[65] M. Orlandea,[29] J. M. Otalora Goicochea,[2] P. Owen,[53] A. Oyanguren,[64] B. K. Pal,[59] A. Palano,[13,p] F. Palombo,[21,q] M. Palutan,[18] J. Panman,[38] A. Papanestis,[49,38] M. Pappagallo,[51] L. L. Pappalardo,[16,b] C. Parkes,[54] C. J. Parkinson,[9,45] G. Passaleva,[17] G. D. Patel,[52] M. Patel,[53] C. Patrignani,[19,j] A. Pazos Alvarez,[37] A. Pearce,[54] A. Pellegrino,[41] M. Pepe Altarelli,[38] S. Perazzini,[14,h] E. Perez Trigo,[37] P. Perret,[5] M. Perrin-Terrin,[6] L. Pescatore,[45] E. Pesen,[66] K. Petridis,[53] A. Petrolini,[19,j] E. Picatoste Olloqui,[36] B. Pietrzyk,[4] T. Pilař,[48] D. Pinci,[25] A. Pistone,[19] S. Playfer,[50] M. Plo Casasus,[37] F. Polci,[8] A. Poluektov,[48,34] E. Polycarpo,[2] A. Popov,[35] D. Popov,[10] B. Popovici,[29] C. Potterat,[2] E. Price,[46]

J. Prisciandaro,[39] A. Pritchard,[52] C. Prouve,[46] V. Pugatch,[44] A. Puig Navarro,[39] G. Punzi,[23,r] W. Qian,[4] B. Rachwal,[26] J. H. Rademacker,[46] B. Rakotomiaramanana,[39] M. Rama,[18] M. S. Rangel,[2] I. Raniuk,[43] N. Rauschmayr,[38] G. Raven,[42] S. Reichert,[54] M. M. Reid,[48] A. C. dos Reis,[1] S. Ricciardi,[49] S. Richards,[46] M. Rihl,[38] K. Rinnert,[52] V. Rives Molina,[36] D. A. Roa Romero,[5] P. Robbe,[7] A. B. Rodrigues,[1] E. Rodrigues,[54] P. Rodriguez Perez,[54] S. Roiser,[38] V. Romanovsky,[35] A. Romero Vidal,[37] M. Rotondo,[22] J. Rouvinet,[39] T. Ruf,[38] F. Ruffini,[23] H. Ruiz,[36] P. Ruiz Valls,[64] J. J. Saborido Silva,[37] N. Sagidova,[30] P. Sail,[51] B. Saitta,[15,m] V. Salustino Guimaraes,[2] C. Sanchez Mayordomo,[64] B. Sanmartin Sedes,[37] R. Santacesaria,[25] C. Santamarina Rios,[37] E. Santovetti,[24,i] A. Sarti,[18,s] C. Satriano,[25,c] A. Satta,[24] D. M. Saunders,[46] M. Savrie,[16,b] D. Savrina,[31,32] M. Schiller,[42] H. Schindler,[38] M. Schlupp,[9] M. Schmelling,[10] B. Schmidt,[38] O. Schneider,[39] A. Schopper,[38] M.-H. Schune,[7] R. Schwemmer,[38] B. Sciascia,[18] A. Sciubba,[25] M. Seco,[37] A. Semennikov,[31] I. Sepp,[53] N. Serra,[40] J. Serrano,[6] L. Sestini,[22] P. Seyfert,[11] M. Shapkin,[35] I. Shapoval,[16,43,b] Y. Shcheglov,[30] T. Shears,[52] L. Shekhtman,[34] V. Shevchenko,[63] A. Shires,[9] R. Silva Coutinho,[48] G. Simi,[22] M. Sirendi,[47] N. Skidmore,[46] T. Skwarnicki,[59] N. A. Smith,[52] E. Smith,[55,49] E. Smith,[53] J. Smith,[47] M. Smith,[54] H. Snoek,[41] M. D. Sokoloff,[57] F. J. P. Soler,[51] F. Soomro,[39] D. Souza,[46] B. Souza De Paula,[2] B. Spaan,[9] A. Sparkes,[50] P. Spradlin,[51] S. Sridharan,[38] F. Stagni,[38] M. Stahl,[11] S. Stahl,[11] O. Steinkamp,[40] O. Stenyakin,[35] S. Stevenson,[55] S. Stoica,[29] S. Stone,[59] B. Storaci,[40] S. Stracka,[23,38] M. Straticiuc,[29] U. Straumann,[40] R. Stroili,[22] V. K. Subbiah,[38] L. Sun,[57] W. Sutcliffe,[53] K. Swientek,[27] S. Swientek,[9] V. Syropoulos,[42] M. Szczekowski,[28] P. Szczypka,[39,38] D. Szilard,[2] T. Szumlak,[27] S. T'Jampens,[4] M. Teklishyn,[7] G. Tellarini,[16,b] F. Teubert,[38] C. Thomas,[55] E. Thomas,[38] J. van Tilburg,[41] V. Tisserand,[4] M. Tobin,[39] S. Tolk,[42] L. Tomassetti,[16,b] D. Tonelli,[38] S. Topp-Joergensen,[55] N. Torr,[55] E. Tournefier,[4] S. Tourneur,[39] M. T. Tran,[39] M. Tresch,[40] A. Tsaregorodtsev,[6] P. Tsopelas,[41] N. Tuning,[41] M. Ubeda Garcia,[38] A. Ukleja,[28] A. Ustyuzhanin,[63] U. Uwer,[11] V. Vagnoni,[14] G. Valenti,[14] A. Vallier,[7] R. Vazquez Gomez,[18] P. Vazquez Regueiro,[37] C. Vázquez Sierra,[37] S. Vecchi,[16] J. J. Velthuis,[46] M. Veltri,[17,t] G. Veneziano,[39] M. Vesterinen,[11] B. Viaud,[7] D. Vieira,[2] M. Vieites Diaz,[37] X. Vilasis-Cardona,[36,g] A. Vollhardt,[40] D. Volyanskyy,[10] D. Voong,[46] A. Vorobyev,[30] V. Vorobyev,[34] C. Voß,[62] H. Voss,[10] J. A. de Vries,[41] R. Waldi,[62] C. Wallace,[48] R. Wallace,[12] J. Walsh,[23] S. Wandernoth,[11] J. Wang,[59] D. R. Ward,[47] N. K. Watson,[45] D. Websdale,[53] M. Whitehead,[48] J. Wicht,[38] D. Wiedner,[11] G. Wilkinson,[55] M. P. Williams,[45] M. Williams,[56] F. F. Wilson,[49] J. Wimberley,[58] J. Wishahi,[9] W. Wislicki,[28] M. Witek,[26] G. Wormser,[7] S. A. Wotton,[47] S. Wright,[47] S. Wu,[3] K. Wyllie,[38] Y. Xie,[61] Z. Xing,[59] Z. Xu,[39] Z. Yang,[3] X. Yuan,[3] O. Yushchenko,[35] M. Zangoli,[14] M. Zavertyaev,[10,u] L. Zhang,[59] W. C. Zhang,[12] Y. Zhang,[3] A. Zhelezov,[11] A. Zhokhov,[31] L. Zhong[3] and A. Zvyagin[38]

(LHCb Collaboration)

[1]*Centro Brasileiro de Pesquisas Físicas (CBPF), Rio de Janeiro, Brazil*
[2]*Universidade Federal do Rio de Janeiro (UFRJ), Rio de Janeiro, Brazil*
[3]*Center for High Energy Physics, Tsinghua University, Beijing, China*
[4]*LAPP, Université de Savoie, CNRS/IN2P3, Annecy-Le-Vieux, France*
[5]*Clermont Université, Université Blaise Pascal, CNRS/IN2P3, LPC, Clermont-Ferrand, France*
[6]*CPPM, Aix-Marseille Université, CNRS/IN2P3, Marseille, France*
[7]*LAL, Université Paris-Sud, CNRS/IN2P3, Orsay, France*
[8]*LPNHE, Université Pierre et Marie Curie, Université Paris Diderot, CNRS/IN2P3, Paris, France*
[9]*Fakultät Physik, Technische Universität Dortmund, Dortmund, Germany*
[10]*Max-Planck-Institut für Kernphysik (MPIK), Heidelberg, Germany*
[11]*Physikalisches Institut, Ruprecht-Karls-Universität Heidelberg, Heidelberg, Germany*
[12]*School of Physics, University College Dublin, Dublin, Ireland*
[13]*Sezione INFN di Bari, Bari, Italy*
[14]*Sezione INFN di Bologna, Bologna, Italy*
[15]*Sezione INFN di Cagliari, Cagliari, Italy*
[16]*Sezione INFN di Ferrara, Ferrara, Italy*
[17]*Sezione INFN di Firenze, Firenze, Italy*
[18]*Laboratori Nazionali dell'INFN di Frascati, Frascati, Italy*
[19]*Sezione INFN di Genova, Genova, Italy*
[20]*Sezione INFN di Milano Bicocca, Milano, Italy*
[21]*Sezione INFN di Milano, Milano, Italy*
[22]*Sezione INFN di Padova, Padova, Italy*
[23]*Sezione INFN di Pisa, Pisa, Italy*
[24]*Sezione INFN di Roma Tor Vergata, Roma, Italy*

[25]Sezione INFN di Roma La Sapienza, Roma, Italy
[26]Henryk Niewodniczanski Institute of Nuclear Physics Polish Academy of Sciences, Kraków, Poland
[27]AGH—University of Science and Technology, Faculty of Physics and Applied Computer Science, Kraków, Poland
[28]National Center for Nuclear Research (NCBJ), Warsaw, Poland
[29]Horia Hulubei National Institute of Physics and Nuclear Engineering, Bucharest-Magurele, Romania
[30]Petersburg Nuclear Physics Institute (PNPI), Gatchina, Russia
[31]Institute of Theoretical and Experimental Physics (ITEP), Moscow, Russia
[32]Institute of Nuclear Physics, Moscow State University (SINP MSU), Moscow, Russia
[33]Institute for Nuclear Research of the Russian Academy of Sciences (INR RAN), Moscow, Russia
[34]Budker Institute of Nuclear Physics (SB RAS) and Novosibirsk State University, Novosibirsk, Russia
[35]Institute for High Energy Physics (IHEP), Protvino, Russia
[36]Universitat de Barcelona, Barcelona, Spain
[37]Universidad de Santiago de Compostela, Santiago de Compostela, Spain
[38]European Organization for Nuclear Research (CERN), Geneva, Switzerland
[39]Ecole Polytechnique Fédérale de Lausanne (EPFL), Lausanne, Switzerland
[40]Physik-Institut, Universität Zürich, Zürich, Switzerland
[41]Nikhef National Institute for Subatomic Physics, Amsterdam, The Netherlands
[42]Nikhef National Institute for Subatomic Physics and VU University Amsterdam, Amsterdam, The Netherlands
[43]NSC Kharkiv Institute of Physics and Technology (NSC KIPT), Kharkiv, Ukraine
[44]Institute for Nuclear Research of the National Academy of Sciences (KINR), Kyiv, Ukraine
[45]University of Birmingham, Birmingham, United Kingdom
[46]H.H. Wills Physics Laboratory, University of Bristol, Bristol, United Kingdom
[47]Cavendish Laboratory, University of Cambridge, Cambridge, United Kingdom
[48]Department of Physics, University of Warwick, Coventry, United Kingdom
[49]STFC Rutherford Appleton Laboratory, Didcot, United Kingdom
[50]School of Physics and Astronomy, University of Edinburgh, Edinburgh, United Kingdom
[51]School of Physics and Astronomy, University of Glasgow, Glasgow, United Kingdom
[52]Oliver Lodge Laboratory, University of Liverpool, Liverpool, United Kingdom
[53]Imperial College London, London, United Kingdom
[54]School of Physics and Astronomy, University of Manchester, Manchester, United Kingdom
[55]Department of Physics, University of Oxford, Oxford, United Kingdom
[56]Massachusetts Institute of Technology, Cambridge, Massachusetts 02142, USA
[57]University of Cincinnati, Cincinnati, Ohio 45220, USA
[58]University of Maryland, College Park, Maryland 20742, USA
[59]Syracuse University, Syracuse, New York 13244, USA
[60]Pontifícia Universidade Católica do Rio de Janeiro (PUC-Rio), Rio de Janeiro, Brazil
(associated with Universidade Federal do Rio de Janeiro (UFRJ), Rio de Janeiro, Brazil)
[61]Institute of Particle Physics, Central China Normal University, Wuhan, Hubei, China
(associated with Center for High Energy Physics, Tsinghua University, Beijing, China)
[62]Institut für Physik, Universität Rostock, Rostock, Germany
(associated with Physikalisches Institut, Ruprecht-Karls-Universität Heidelberg, Heidelberg, Germany)
[63]National Research Centre Kurchatov Institute, Moscow, Russia
(associated with Institute of Theoretical and Experimental Physics (ITEP), Moscow, Russia)
[64]Instituto de Fisica Corpuscular (IFIC), Universitat de Valencia-CSIC, Valencia, Spain
(associated with Universitat de Barcelona, Barcelona, Spain)
[65]KVI–University of Groningen, Groningen, The Netherlands
(associated with Nikhef National Institute for Subatomic Physics, Amsterdam, The Netherlands)
[66]Celal Bayar University, Manisa, Turkey
(associated with European Organization for Nuclear Research (CERN), Geneva, Switzerland)

[a]Also at Università di Firenze, Firenze, Italy.
[b]Also at Università di Ferrara, Ferrara, Italy.
[c]Also at Università della Basilicata, Potenza, Italy.
[d]Also at Università di Modena e Reggio Emilia, Modena, Italy.
[e]Also at Università di Padova, Padova, Italy.
[f]Also at Università di Milano Bicocca, Milano, Italy.
[g]Also at LIFAELS, La Salle, Universitat Ramon Llull, Barcelona, Spain.
[h]Also at Università di Bologna, Bologna, Italy.
[i]Also at Università di Roma Tor Vergata, Roma, Italy.
[j]Also at Università di Genova, Genova, Italy.

[k]Also at Universidade Federal do Triângulo Mineiro (UFTM), Uberaba-MG, Brazil.
[l]Also at AGH—University of Science and Technology, Faculty of Computer Science, Electronics and Telecommunications, Kraków, Poland.
[m]Also at Università di Cagliari, Cagliari, Italy.
[n]Also at Scuola Normale Superiore, Pisa, Italy.
[o]Also at Hanoi University of Science, Hanoi, Viet Nam.
[p]Also at Università di Bari, Bari, Italy.
[q]Also at Università degli Studi di Milano, Milano, Italy.
[r]Also at Università di Pisa, Pisa, Italy.
[s]Also at Università di Roma La Sapienza, Roma, Italy.
[t]Also at Università di Urbino, Urbino, Italy.
[u]Also at P.N. Lebedev Physical Institute, Russian Academy of Science (LPI RAS), Moscow, Russia.